

Production and Characterization of Plastic-Rice Husk Based Membrane for the Ultra-Filtration of Oily Wastewater

Chidinma F. Akaeme*, Matthew C. Menkiti, Chijioke E. Onu

Department of Chemical Engineering, Nnamdi Azikiwe University, Awka, Anambra State

✉: cf.akaeme@unizik.edu.ng; +2348133932313

Received: 18.09.2023

Accepted: 16.10.2023

Published: 19.10.2023

Abstract:

This work focuses on the synthesis and characterization of Polyethylene terephthalate/ Polyethylene glycol/Carbonized rice husk ash (PET/PEG/CRHA) membrane for the ultra-filtration of oil wastewater. The polymer membrane was modified with varied concentrations of carbonized rice husk ash (CRHA) through the blending method of modification to produce Flat Sheet Membrane (FSM) samples. These FSM samples were characterized to determine their surface morphology, functional groups present, thermal and mechanical stability as well as the hydrophilicity of the membranes. Similarly, the membranes were also characterized for their porosity, water content, flux (both permeate and pure water) and % oil rejection ability. The results indicate that addition of CRHA into dope membrane solution greatly influenced the morphological and performance characteristics of produced FSM samples. The highest thickness, porosity and water adsorption capacity of 0.48 cm, 36.22 % and 53.17 % were obtained for FSM5, FSM4 and FSM2 respectively, while the least values of 8.72 Mpa, 4.15 %, and 400 °C for tensile strength, elongation at break, and thermal strength were obtained for FSM1. FSM4 performed optimally well when compared with other membrane samples. FSM4 recorded the highest pure water flux of 1500 L/m²h, permeate flux of 813.8 L/m².h and second highest value for percentage oil rejection of 69.42 % at a pressure of 3.0 bar and filtration time of 20 min. Hence, low-cost ultra-filtration membrane with improved permeate flux and % oil rejection can be synthesized from waste PET bottles by the addition of PEG and CRHA as pore forming additives.

Keywords: Flat sheet membrane (FSM), Oily wastewater treatment, Polyethylene terephthalate (PET), Rice husk (RH), Ultra-filtration process

1. Introduction

Nigeria as a country has recorded growth in its industrial sector in the last few years, with petroleum and chemical industry ranking among the leading sectors. However, improperly treated liquid wastes discharged by these industries is associated with harmful effects on human health, environment, and ecological systems, with oily wastewater having the highest lead [1]. The magnitude of oil pollution has grown rapidly over the years due to increased number of oil based factories (crude oil refineries, petrochemicals and thermal/chemical plants, service stations etc) in the country [2]. According to NOSDRA between January 2006 and June 2021, a total of 14,693 oil spillage events happened in Nigeria [3]. This is equivalent to 738,083 barrels (116.4 million litres) of oil wasted on lands and water bodies, within this period. It has become certain that this act cannot be totally avoided and may continue to increase with increasing number of oil based industries in the country. Hence, the need to impose the implementation of waste treatment, reuse, and discharge limits by regulatory bodies [1].

Some techniques for treating oil wastewater include adsorption, coagulation, flocculation centrifuges, electrochemical and photocatalytic treatment [4]. However, the aforementioned techniques have some drawbacks in the areas of minimal separation performance, high cost, complicated operational handling (in some situations), and most crucially generation of additional pollutants and failure in separating oil wastewater

with less than 10 mm particle sizes [5,6]. To ensure continued technological advancement and a healthy environment, it is imperative to create environmental friendly, effective, and dependable technology [7].

Technology based on membranes principle has become a viable alternative [4]. The benefits of this method (membrane) over others include excellent oil removal, ease of design, a reduced need for chemical additives [8], and stable effluent quality [9], but it is mainly faced with the problem of membrane fouling. These days, polymers are the most studied membrane materials because of their outstanding properties (flexibility, mechanical and chemical stability). Commercial polymers are very expensive and polymeric membranes are easily fouled, hence, the need to embark on polymeric membrane modification (to reduce/eliminate membrane fouling) and achieve substitution of expensive commercial polymers for the successful treatment of oil wastewater.

Polyethylene terephthalate (PET) is extremely stable at high temperatures and has a strong, long-lasting structure. These characteristics made PET difficult to breakdown in the environment [10]. The frequent use of PET for food and beverage packaging has resulted to the generation of PET-based plastic bottle waste, which its poor disposal is causing environmental pollution. Nigeria rank tenth among the nations that contribute the most to plastic pollution worldwide [11]. Sadly, not more than 8% of Nigeria's plastic garbage is recycled; majority of it ends up in the country's rivers, lakes, sewers, lagoons, and oceans [11]. Nevertheless, waste PET

bottles can be potentially recycled to beneficiate its content as the primary raw material for the production of polymeric membranes. This will help to reduce waste generation, as well as membrane production costs [12]. This would both protect and conserve our naturally resources.

Rajesh and Murthy had earlier reported on the creation of PET membrane from used plastic bottles [13]. The final membrane's mechanical and antifouling qualities were poor. Consequently, a further alteration is required to enhance its qualities. One of the most appealing ways to prevent membrane fouling is to increase the hydrophilic nature of the membrane surface. This reduces the contact between the foulant (oil droplet) and the membrane surface and, as a result, lowers the foulant deposition on the membrane surface. Numerous studies have demonstrated that enhancing the hydrophilicity of membrane surface effectively increases its ability to permeate water while reducing the deposition of oil droplet on the surface of the membrane, thereby, reducing membrane fouling [14]. The most basic form of membrane modification is polymer blending with hydrophilic materials, its produces membrane with more stable and consistent structure. Some hydrophilic materials, such as hydrous manganese dioxide nanoparticles, [15], pluronic F127 [16], and polyethylene glycol/aluminum oxide (PEG/Al₂O₃) [17] have been used by several researchers for this purpose. Additionally, nanoparticles like silicon dioxide (SiO₂), iron oxide (Fe₃O₄), aluminum oxide (Al₂O₃), zirconium dioxide (ZrO₂), titanium dioxide (TiO₂), and zinc oxide (ZnO) affects the resulting membrane's characteristics [18]. The presence of silica functional group can improve the hydrophilicity of polymeric membranes and lessen membrane surface fouling [19]. Both chemical silica, and silica obtained from natural products (such as rice husk silica) have been applied for this purpose [20].

Due to its capacity to create hydroxyl (OH) bonds and its low water toxicity, nano silica has a significant potential to effectively reject oil molecules and allow water to permeate through during filtration. As a result, silica is regarded as a great addition for membrane production. Rice husk is an abundant natural source of silica [21]. In Nigeria about 2.0 million tons of rice is produced annually. Approximately, 20kg of rice husk are obtained from 100kg of rice [22]. Its burning generates rice husk ash (RHA), which is rich in silica and can be used as an economic and sustainable source of additive in membrane fabrication. Presently, rice farmers are faced with paucity of disposal space, hence their resort to burning of the rice husk, and consequent release of harmful pollutant (carbon monoxide) into the environment. This study will present an opportunity for an eco-friendly method of rice husk disposal, while it addresses the problem of oil wastewater treatment through membrane filtration.

Polyethylene glycol (PEG) was used as a co additive to facilitate the formation of hydrophilic membrane. PEG has been reported to greatly enhance the hydrophilicity of polymer membranes [23,24]. RHA was also used to enhance the hydrophilic and pore characteristics of PET/PEG-based membranes. Currently, no work has been reported on the synthesis of PET/PEG/CRHA hybrid membrane for the

ultrafiltration of oily wastewater except finding from this study. Therefore, it is aimed in this work to synthesize and characterize PET/PEG/CRHA membrane using different concentrations of rice husk ash. Thermally induced phase separation (TIPS) technique was adopted in membrane synthesis.

2. Materials and Methods

2.1 Materials

Polyethylene terephthalate (PET) as the basic polymer was obtained from waste plastic bottles. The plastic bottles were picked from waste dump site located at Okpuno Awka, Anambra State, while the rice husk waste was sourced from a local rice threshing mills in Ajalli, Anambra State. The rice husk was sun-dried for 2-3 days and then stored in a sack bag under room temperature until usage. The reagents (phenol, ethanol and distilled water) used were of analytical grade at 99 % purity and were sourced from reputable chemical vendors located at main market in Onitsha, Anambra state..

2.2 Preparation of carbonized rice husk

500 g of rice husks was weighed and washed with tap water and distilled water, respectively until the water is clear. Then it was oven (Nemert Oven Din 40050-Ip20) dried for 8 hrs at 105 °C. This is named as raw rice husk (RRH). The RRH was carbonized in muffle furnace (PT- 1400M) at 600 °C for 3 hrs. The black coloured carbonized RRH (CRRH) obtained was further washed with distilled water and oven dried again. The oven-dried CRRH was subsequently reduced in size (to produce carbonized rice husk ash (CRHA)) using electric grinder and stored in sealed polyethylene bags to be used as additive for the experiment.

2.3 Preparation of membrane

The PET polymer used in this work was obtained from waste plastic bottles. First, the labels and bottle caps were removed and the bottles thoroughly washed. The clean and dry plastic bottles (majorly PET content) were then shredded to obtain small pieces of polymer. Next, phenol was liquefied at 40 °C. The polymer-based PET, together with the PEG 450 and varying concentrations of CRHA additive was altogether dissolved in the liquefied phenol solvent at a temperature of 80 °C using hot plate (Electric Hot Plate DB – 1A), equipped with a magnetic stirrer (Gallenkamp Magnetic stirrer and Regulator Hotplate). The resulting mixture was stirred until homogeneity is achieved to produce the casting solution (CASOL). In order to produce desired varying CASOL samples, the formulations depicted in Table 1 below was reproduced. Each of the CASOL sample was poured on a petri dish to produce casting film. This film was allowed to evaporate for about 20 sec and; then immersed in a bath containing water-ethanol (as a non-solvent) in the ratio of 15:1 [10] at room temperature to produce flat sheet membrane (FSM). Subsequently, the produced FSM was rinsed severally with distilled water and allowed to properly dry before further use.

Table 1: Composition of membrane formation Solution [23]

Membrane	PET/Phenol /PEG	CRHA (wt%)
FSM 1	4:20:2	0
FSM 2	4:20:2	2.0
FSM 3	4:20:2	3.0
FSM 4	4:20:2	4.0
FSM 5	4:20:2	5.0

2.4 Synthetic wastewater preparation

Crude oil-water emulsion of 1000 ppm oil concentration in the distilled water was prepared by mixing (in a container) calculated amount of crude oil with distilled water for 24 hrs. Then, a homogenizer (KIKA Labortechnik) was used to achieve equilibrium between the oil and water phases

2.5 Characterization of PET/PEG/CRHA membrane

The FSM samples were characterized based on their morphological and performance properties as follow:

2.5.1 Scanning electron microscopy (SEM)

Each sample of the FSM was subjected to SEM analysis (SEM, Hitachi SU 3500 scanning microscope, Tokyo, Japan) to study the surface morphology according to ASTM E2809 (2013). FSM sample was prepared by cleaning the surface, rinsing, drying and coating the sample with gold of about 20 nm thickness. The main objective of coating the sample is to increase its conductivity and to provide the buildup of high voltage charges on the specimen. Energy Dispersive X-ray Spectroscopy (SEM-EDX) was also utilized in the analysis in order to eliminate the effect of sample contamination due to the presence of external substances on membrane surface, which may affect the quality of the samples.

2.5.2 Fourier-transform infrared spectroscopy (FTIR)

FTIR spectroscopy was conducted based on ASTM E168 (2016), in order to investigate the functional groups present in the membrane samples. About 4 mg (in powder) of each sample was mixed with potassium bromide in the ratio of 1 to 100. In order to create a pellet (< 15mm thick), the mixture was forced through a die at a load of 10 tons. The pellet is next put into the FTIR chamber for analysis. Potassium bromide is frequently used because it does not interfere in the infrared window between wavelength of 400 cm⁻¹ to 4000 cm⁻¹. The spectra were recorded within the frequency range of 4000 cm⁻¹ to 500 cm⁻¹ using an FT-IR spectrometer (Infrared spectrometer Varian 660 MidIR Dual MCT/DTGS Bundle with ATR)) with a detector at 4 cm⁻¹ resolution and 200 scans per sample. The refractogram obtained from FT-IR spectrometer between the stated wave numbers and absorption band was tabulated. IR solution software was employed in getting the spectrum.

2.5.3 Thermogravimetric analysis (TGA)

According to ASTM D3418 (2015), the thermal stability of FSM samples were evaluated using a TGA (Shimadzu TGA - Q50 thermobalance) thermal analyzer. Prior to TGA, the membrane samples were pre-dried at 60 oC overnight. The temperature range of 30 oC to 700 oC was used to measure the

thermal degradation of membrane samples. This procedure was carried out in a nitrogen atmosphere at a heating rate of 10 °C/min and 10 mL/min.

2.5.4 Porosity

Equation (1) was used to determine membrane porosity [25]:

$$\varepsilon (\%) = \frac{(W_w - W_d)}{fA\delta} \quad (1)$$

where :

W_w and W_d are the weight of the wet and dry membrane samples, respectively, f, A and δ are the density of the water (g/cm³), the surface area of FSM sample (cm²) and the thickness of wet membrane sample (cm) respectively.

The FSM samples were placed in distilled deionized water at room temperature for 24 hours to produce the wet membrane, then for 2 hours at 100 °C to produce the dry membrane. The average value of the porosity was calculated after analysis of five distinct samples from each FSM sample.

2.5.5 Water contact angle

Water contact angle meter was used to analyze the hydrophilicity of the FSM sample. The test substance (distilled water) was partially submerged in the samples. Then the goniometer with the optical camera was used to monitor the meniscus. Following the achievement of the equilibrium condition, contact angles were measured. This was accomplished by gradually varying the test liquid level in the container that samples were partially submerged. Every measurement was made at room temperature. Three different measurements were made and the average value taken. In all cases, contact angle data was reported in terms of water contact angle (°).

2.5.6 Water content

This was performed to study the water absorption capacity of FSM samples. Dried membrane was cut into 1cm (width) x 1cm (length), weighed and immersed in distilled water at room temperature for 24 hrs. Then, the wet membranes were removed, wiped with filter paper to remove excess water on membrane surfaces and their weight taken again with the aid of a weighing balance. This was repeated five different times for each FSM sample. The water content was calculated based on equation (2) [25]

$$\text{water content } (\%) = \frac{W_w - W_d}{W_w} \times 100\% \quad (2)$$

2.5.7 Mechanical Properties

Each FSM sample was tested for the mechanical properties using a universal tensile tester (ELE International, Loveland, Colorado, USA) in accordance with the ASTM D882 (2021) standard. Each sample was divided into 50 mm long and 15 mm wide. About 50 mm/min crosshead speed was chosen. Each sample's thickness ranged from 0.2 mm to 0.5 mm. At room

temperature, the tensile strength (MPa) and elongation at break (%) were measured.

2.5.8 Pure water flux

Pure water flux was investigated using dead-end filtering machine (adapted from ASTM-E1343; 2001). The membrane holder was positioned with a clean membrane on it, and 0.5 L of distilled water was introduced into the filtration apparatus. The filtration was run for 30 minutes at pressures ranging from 0.5 bar to 2.5 bar. The pure permeate flux was determined using equation 3 [23]. At each pressure, three different measurements were made and the average taken.

$$\text{Flux (L/m}^2\text{h)} = \frac{V}{A.t} \quad (3)$$

Where

V is the volume of permeate (L)

A the effective surface area of the membrane (m²)

t filtration time (h).

2.6 Oily wastewater filtration experiment

Synthesized oily wastewater was treated using dead-end filtration as well. The oily wastewater filtration efficiency was monitored through reduction in the oil content of wastewater. The concentration of oil in the synthesized wastewater before and after filtration was analyzed using a Spectrophotometer (BUCK Scientific Infrared Spectrophotometer Model 910); according to the ASTM E 168 (2016) method at a wavelength of 750nm. The amount of oil rejected by the FSM samples at different filtration time was calculated using Equation (4) [24].

$$\text{Oil rejection(\%)} = \left(1 - \frac{C_p}{C_f}\right) * 100 \quad (4)$$

Where

C_p indicates concentration of oil in the product solution

C_f indicates the concentration of oil in the feed solution

Every experiment was repeated three times and the average value was reported with standard deviation.

3. Results and Discussion

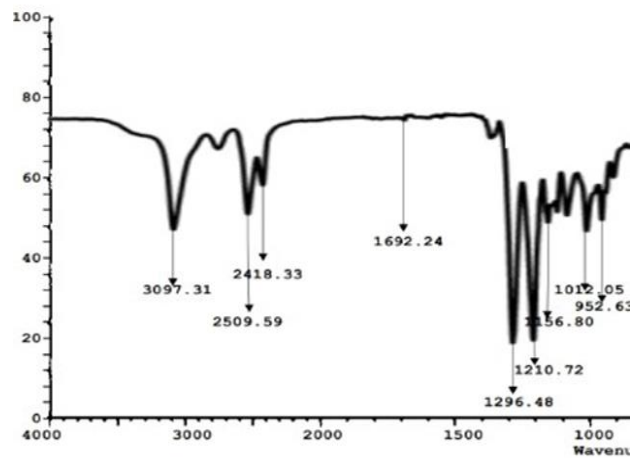
3.1 Morphological characterization of PET/PEG/CRHA membrane

3.1.1 Fourier Transform Infrared (FTIR) Analysis of PET/PEG/CRHA membrane

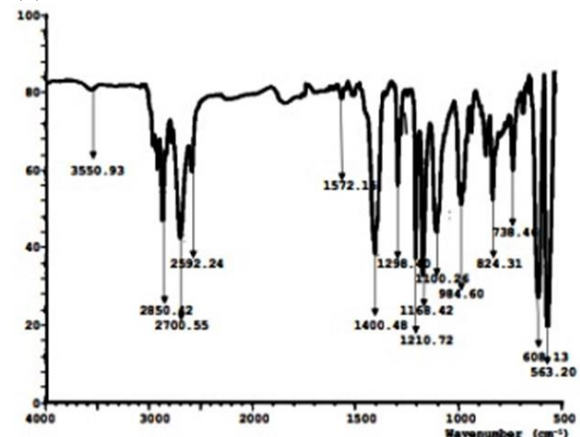
The surface chemistry of FSM samples were analyzed using FTIR spectroscopy in order to determine the functional groups present in each sample. Fig. 1(a – e) below shows the spectra of membrane samples synthesized from waste PET bottles and PEG 450 using CRHA of different concentrations (FSM1, FSM2, FSM3, FSM4 and FSM5) as additive. FTIR spectra over wave number of 4000 cm⁻¹ – 500 cm⁻¹ were presented. The membrane samples with or without CRHA blends had peaks at 3550.93 cm⁻¹ and 3097.31 cm⁻¹ indicating Si-OH and O-H bond of the hydroxyl groups respectively, while the peaks at

2850.42 cm⁻¹ and 1400.48 cm⁻¹ were due to the C-H groups of PET and CRHA. Furthermore, vibration peaks at 1296.48 cm⁻¹, 1210.72 cm⁻¹, 1168.42 cm⁻¹, 1156.80 cm⁻¹ and 1012.05 cm⁻¹ identify C-O stretching of the terephthalate group [26]. The peak at 2418.33 cm⁻¹ was assignable to stretching vibration of the carbonates group. Additionally, peaks at 2509.59 cm⁻¹, 2592.24 cm⁻¹ and 1692.24 cm⁻¹ were associated to stretching vibration of the C=O group. The stretching vibration at 1572.15 cm⁻¹ was as a result of the C-C group. Meanwhile, the addition of PEG into the polymer solution was identified by a vibration peaks at 3500 cm⁻¹ and 2700.55 cm⁻¹ indicating the presence of C-O bond of the ester group [27]. For the CRHA-blended membranes, the appearance of little peak at a wave number of 1572.15 cm⁻¹ was attributed to the C=C group while vibration peaks at 1100.26 cm⁻¹, 1012.05 cm⁻¹ and 984.60 cm⁻¹ indicated the presence Si-O-Si group and stretching vibrations at 824.31 cm⁻¹ to 563.20 cm⁻¹ showed the presence of Si-H group from CRHA additive. Similar functional groups were reported by Harun et al., [27] for Psf mixed matrix membrane, and Mulyati et al., [10] for PET/CA/SiO₂ membrane. The presence of SiO₂ functional group in membranes blended with CRHA would enhance the hydrophilicity of PET/PEG/CRHA membrane. Hence, causing the rejection of oil droplet while allowing water to pass through in the ultrafiltration of oily wastewater.

(a)



(b)



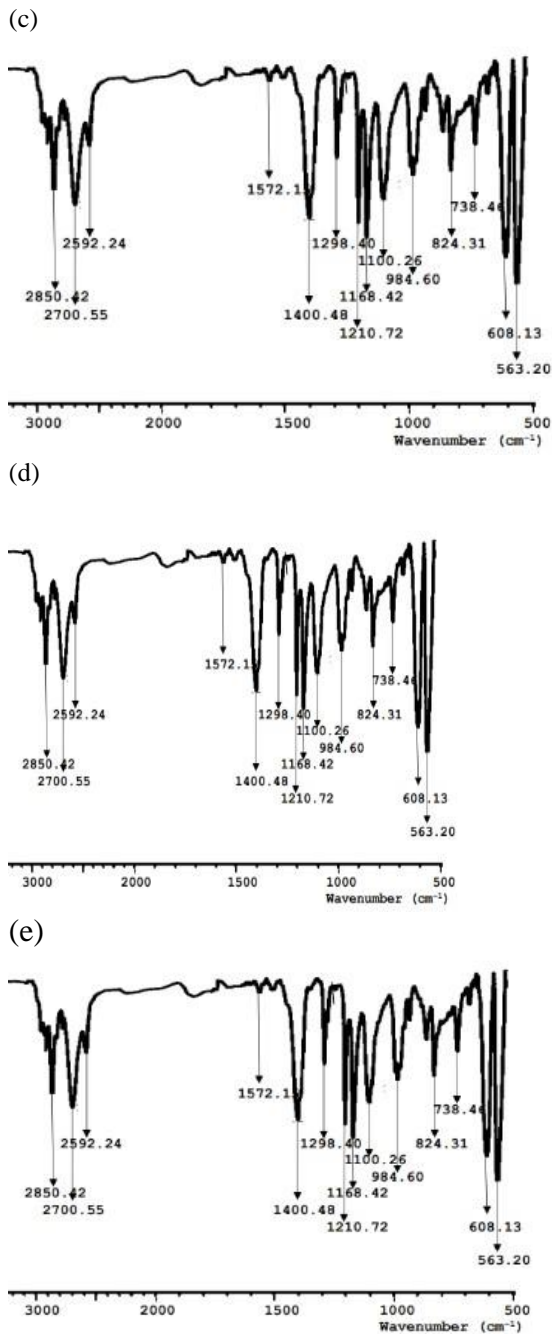


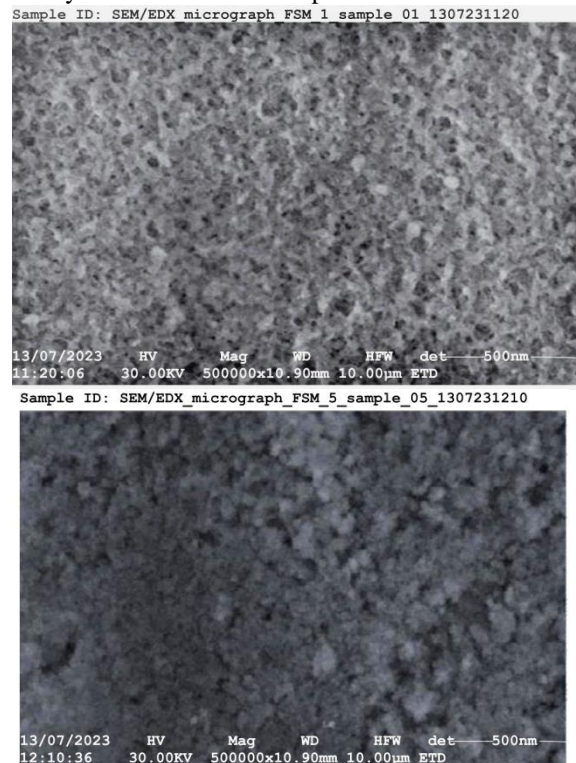
Fig. 1. (a –e): FTIR spectrum of the membrane samples; FSM1, FSM2, FSM3, FSM4 and FSM5 respectively

3.1.2 Scanning electron microscope (SEM) of PET/PEG/CRHA membrane

Fig. 2 shows the SEM images of FSM samples at different concentration of CRHA in the composite membranes. It was observed that CRHA was dispersed uniformly in the FSM samples, giving a typical asymmetric structure, with a dense top layer supported by tear-like structure and a porous spongy sub-layer. The SEM images for the microstructure of the produced FSM showed that increase in the concentration of CRHA resulted to a decrease in the pore size of the membrane cross section but increases the distribution of pores on the surface of

the membrane samples as shown in Fig. 2. Since, CRHA acts as a pore-forming agent [27], its major constituent (silica) has great affinity towards water. This causes the leaching out of CRHA during precipitation process. Therefore, affecting pore formation and distribution on the surface of the FSM samples [10]. Similarly, Muhamad et al., [28], reported in his work that the presence of SiO₂ functional group tends to decrease the thermodynamic stability of the process during membrane production, causing the liquid-liquid phase separation to occur more quickly and produce more pores on the membrane surfaces. Increasing the concentration of CRHA increases the porosity of FSM samples. This is in agreement with the results reported by Harun et al., [27] in the synthesizes of polysulfone (PSf) membrane using two different rice husk silica as additives.

At the highest concentration of CRHA (5wt%), The membrane structure appeared to be significantly denser and had fewer pores.. This was due to a decrease in the rate of solvent and non-solvent exchange which suppressed the formation of macropores [25] as a result of increased viscosity of the polymeric solution. Similar phenomenon was also reported by Ahmad et al., [29] who prepared functionalized PSf nanocomposite membrane using SiO₂ as additive. Mulyati et al., [10] again reported that silica obtained from rice husk improved the hydrophilicity of membrane surface, he went further to add that at very high concentration of rice husk silica (1 wt%), the porosity and hydrophilicity of the membrane reduced. With increased porosity and hydrophilicity, membrane permeate flux and oil rejection tend to increase as membrane fouling decreases drastically, thus improving the performance of oily wastewater filtration process.



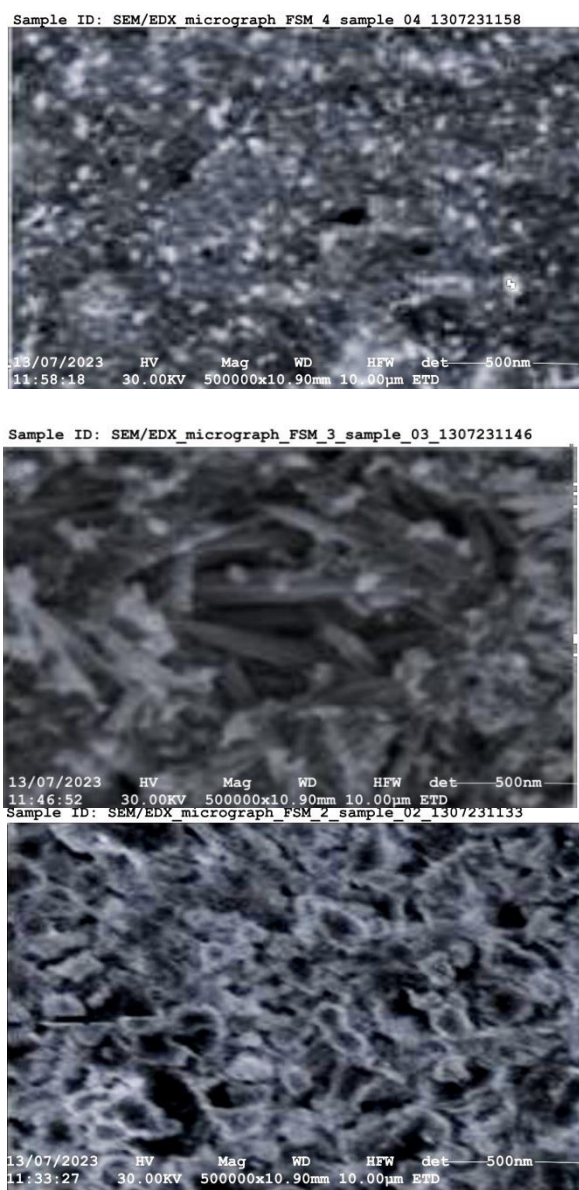


Fig. 2. SEM-EDX images of FSM1, FMS2, FMS3, FMS4 and FMS5 respectively.

3.1.3 Thermogravimetric analysis (TGA) of PET/PEG/CRHA membrane

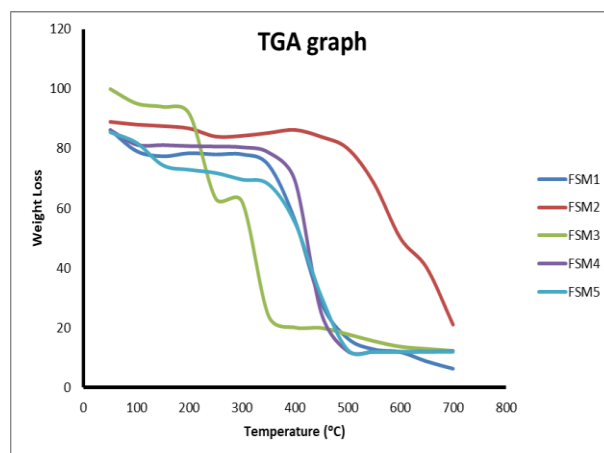
TGA study was conducted on the synthesized FSM samples to validate the thermal property of the produced membranes at heating rate of 20 °C/min–50 °C/min. The TGA and derivative thermogravimetric (DTG) curves for the various membranes produced using varying CRHA concentrations are shown in Fig. 3. The DTG curves recorded one identifiable peak for a temperature range of 50 °C -700 °C, whereas the TGA curves for the various membrane samples revealed two (for FSM2) and three (FSM1, FSM3, FSM4 and FSM5) phases of weight loss. Similar TGA results was reported by Kiani et al., [25] during the thermal decomposition of PET/XA membrane. Also Nalatambi et al., [30] and Gola et al., [31] both reported three weight loss stages for CS/GO membranes and poly-N-

Isopropylacrylamide (PNIPA) membranes respectively.

The first stage of weight loss was attributed to the evaporation of absorbed water and residual solvent which occurred within a temperature range of 50 °C – 200 °C. Here, FSM5, FSM4, FSM1 and FSM2 recorded the highest weight loss of 14.64 %, 13.90 % 13.69 % and 11.08 % respectively whereas FSM3 recorded no weight loss within this temperature range. The second stage of weight loss was observed between a temperature range of 200 °C – 400°C and was assigned to the thermal degradation of PET and PEG through depolymerization of PET and elimination of glycosidic unit of PEG. At this stage, the maximum weight loss recorded for FSM1, FSM2, FSM3, FSM4 and FSM5 were 43.87 %, 32.00 %, 33.59 %, 30.79 % and 33.85 % respectively. This is in line with that reported by Kiani et al., [25] for PET/XA membrane and Nalatambi et al., [30] for CS/GO membrane.

Subsequently, the third stage of weight loss for the different membrane samples within the temperature range of 400 °C – 700 °C was as a result of the decomposition of oxygenated functional groups of CRHA. Here, a significant weight loss was recorded for all membrane samples. These include 93.68 % for FSM1, 89.00 % for FSM2, 89.95 % for FSM3, 88.00 % for FSM4 and FSM5. However, it was observed that beyond the decomposition temperature of 500 °C there was no significant change in the mass of FSM4 and FSM5 samples. This indicates the high thermal stability of these samples. Therefore, the residues left after the decomposition of oxygenated functional groups were 6.32 %, 11.00 %, 10.05 %, 12.00 % and 12.00 % for FSM1, FSM2, FSM3, FSM4 and FSM5 respectively.

On the DTG curves of FSM1, FSM2, FSM3, FSM4 and FSM5, one distinct peak was observed, this could be assigned to PET degradation. Kiani et al., [25] and Gola et al., [30] reported similar results for PET/XA and PNIPA membranes. The Tdmax values obtained for the various membrane samples were 400 °C for FSM1, 500 °C for FSM2, 450 °C for FSM3, FSM4 and FSM5. Similar range of Tdmax was reported by Kiani et al., [25] and Gola et al., [30] for PET/XA and PNIPA membranes respectively. Comparing the Tdmax of the different membrane samples, it was observed that CRHA incorporation into the dope membrane solution significantly improved the thermal stability of synthesized membranes.



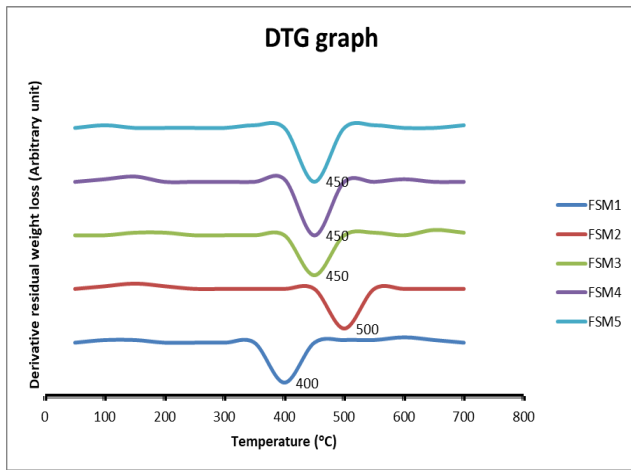


Fig. 3: TGA and DTG of the different membrane samples

3.1.4 Mechanical Properties

This measures the ability of the FSM samples to resist shear pressure during filtration. From literature, PET membranes were reported to have weak mechanical properties [13,16]. The tensile properties of the membrane samples made with different concentrations of CRHA are; presented in Table 2. Addition of CRHA increased the mechanical properties of FSM samples, due to increased concentration of the silica content of CRHA which was observed to increase the membrane porosity and formation of macrovoid in the bulk structure. The highest tensile strength and elongation at break of 40.38 MPa and 10.16 % respectively were reported for FSM4. Similar results were reported by Muhamad et al., [28] and Rojjanapinun & Pagsuyoin [32] for PES modified with SiO₂ and PVDF membrane modified with rice husk ash respectively. Similarly, Kiani et al., [25] and Nalatambi et al., [30] reported a corresponding increase and decrease in mechanical properties as the additive concentration increases. This increase in mechanical properties could be attributed to the high hydrogen bonding between the functional groups of the PET and silica elements. However, it was observed that FSM1 without CRHA loading has the least tensile strength and elongation at break, this is an indication that the addition of CRHA into the membrane solution improved the mechanical stability of the membrane samples. The tensile strength and elongation at break was reported to decrease from 40.38 MPa and 10.16 % for FSM4 to 18.21 MPa and 6.10 % for FSM5. This decrease can be as a result of decrease in membrane porosity noted for FSM5 as the concentration of CRHA increased to 5 wt%, suggesting that further increase in the concentration of CRHA will decrease the mechanical stability of the produced membrane.

Table 2: Mechanical properties of various membrane samples

Samples	Tensile Strength (MPa)	Elongation at Break (%)
FSM1	8.72	4.15
FSM2	21.64	7.85

FSM3	9.23	4.78
FSM4	40.38	10.16
FSM5	18.21	6.10

3.1.5 Porosity

The thickness and porosity of the respective FSM samples are presented in Table 3. The thickness of FSM with different concentrations of CRHA was analyzed using a micrometer. From Table 3, it was observed that addition of CRHA to the membrane structure increased the thickness of the membrane samples, with the maximum thickness of 0.48 cm recorded for FSM5 and the least thickness of 0.27 cm recorded for FSM1. This was attributed to the accelerated solidification observed during membrane formation [33].

While on the other hand, increasing the concentration of CRHA in the polymer solution causes a corresponding decrease and increase in membrane porosity. This trend in membrane porosity can be explained as follow; at first, addition of PEG into the polymer solution increased the porosity of the produced FSM samples as seen in FSM1. Subsequently, adding some concentration of CRHA into PET/PEG solution decreased the pore size but increased the distribution of pores on the surface of FSM samples. So, depending on the concentration of CRHA added to the polymer solution, porosity is either increased or decreased. From Table 3, it was observed that an initial increase in CRHA concentration from 0 wt% - 3 wt% caused a decrease in membrane porosity from 29.26 % to 27.32 % as a result of high membrane solution viscosity, thereby reducing the number of pore space available on the membrane surface. Further increase in CRHA concentration from 3 wt% to 4 wt% led to an increase in membrane porosity, with the highest porosity recorded for FSM4 at 36.22 %. However, the increase in membrane porosity was as a result of increased rates of solvent and non-solvent exchange on account of reduced solution viscosity thus causing an increment in the formation of macropores [25].

So, increasing the concentration of CRHA to 5 wt% in the polymer solution reduced the porosity of the membrane from 36.22 % for FSM4 to 31.60 % for FSM5 by suppressing the formation of macropores on account of increased solution viscosity. Kusumocahyo et al., [24] and Kiani et al., [25] reported similar results for PET membrane blended with PEG400 and XA as additives respectively.

Table 3: Thickness, porosity and water uptake of membrane samples

Samples	Thickness (cm)	Porosity (%)	Water Uptake (%)
FSM1	0.27	29.26	41.82
FSM2	0.28	27.92	53.17
FSM3	0.32	27.32	32.85
FSM4	0.36	36.22	51.04
FSM5	0.48	31.60	49.61

3.1.6 Water content

This measures the ability of the membranes to absorb water.

Porosity and hydrophilicity of membrane have an impact on their ability to absorb water [25,33]. The water content of membranes made with different concentrations of CRHA are shown in Table 3. From Table 3, it was observed that increasing the concentration of CRHA in the FSM samples resulted to a corresponding increase/decrease in the water adsorption capacity of the FSM. This could be attributed to the decrease/increase in membrane porosity as a result of the pore forming ability of the additive. This is in line with the result reported by Kiani et al., [25] for PET membranes modified with Xanthan gum (XA) additive. Also similar results were obtained by Nalatambi et al., [30] for chitosan (CS) membranes using graphene oxide as additive. The highest water adsorption capacity was recorded for FSM2 having a value of 53.17 % as against FSM1 and FSM3 with the least values of 41.82 % and 32.85 % respectively. This could be as a result of the high number of sulfonic acid group present in membranes blended with some concentrations of CRHA. The presence of silica group in membranes blended with CRHA increased the hydrophilic ability of the membrane, this resulted in higher water adsorption capacity recorded for FSM2, FSM4 and FSM5 [34].

3.1.7 Water contact angle (WCA)

Table 4 indicates the WCA of membrane samples prepared in this study. As observed from Table 4, FSM1 have the lowest value of WCA of 70.42°. This was as a result of the hydrophilic nature of PEG added to the membrane structure. PEG as a pore forming agent enhances the porosity of membrane samples [24]. With the addition of CRHA of different concentrations, WCA for FSM2 and FSM3 samples increased to a maximum value of 93.10° for FSM2 and 94.14° for FSM3. Subsequently increasing the concentration of CRHA from 4 wt% to 5 wt% for FSM4 and FSM5, slightly decreased the WCA to 88.44° for FSM4. Therefore, the hydrophilic membrane samples were assigned to FSM1 and FSM2 having WCA of 70.42° and 88.44° respectively. While FSM3, FSM4 and FSM5 are hydrophobic in nature based on the values of their WCA.

The observed increase and decrease in membrane hydrophilicity can be attributed to a corresponding decrease and increase in membrane porosity and pore size distribution noted in membranes with CRHA concentrations (section 3.1.5). Initial concentrations of CRHA (2 wt% and 3 wt%) added to the PET/PEG membrane solution decreased membrane hydrophilicity by increasing the WCA, while further increase in CRHA concentration from 4 wt% to 5 wt% increased the hydrophilicity of the membrane by reducing the WCA. Similar trend was reported by Kiani et al., [25] for higher concentration of XA (1 wt%).

Table 4: Results of the water contact angle for different membrane samples

Samples	Water Contact Angle (°)
FSM1	70.42
FSM2	93.10
FSM3	94.14
FSM4	88.44
FSM5	92.79

3.2 Performance characterization

3.2.1 Pure water flux (PWF)

The pure water flux analysis was conducted to evaluate the ability of water to permeate through the various membrane samples during filtration process at different operating pressure. The filtration was conducted at low pressure ranging from 0.5 bar to 3.0 bar. Table 5 shows the pure water flux of different FSM samples. According to Table 5, the PWF of the various membrane samples increased with increase in operating pressure. FSM1 recorded PWF of 1220.34 L/m²h at a pressure of 3.0 bar. Under similar operating condition, FSM2 and FSM3 recorded a significant decrease in PWF, this could be as a result of the dense structure and the hydrophobic nature of the membrane samples, as well as the decreased membrane porosity. But as the concentration of CRHA increased to 4 wt% and 5 wt% for FSM4 and FSM5 respectively, the PWF also increased, this can be attributed to the improvement of the membrane from its hydrophobic nature (for FSM2 and FSM3) to hydrophilic nature as more hydrophilic groups of CRHA were added into the dope membrane solution.

Based on the results from Table 5, PWF of the various membrane samples were significantly influenced by the concentrations of PEG and CRHA. FSM4 was noted to have the highest PWF of 1500.62 L/m²h, this was due to high membrane porosity recorded for this membrane sample and a shift from hydrophobic membrane to a hydrophilic membrane, making the membrane to have high affinity for water molecules. The PWF of FSM5 was observed to slightly decrease to 1360.30 L/m²h, this could be assigned to decrease in membrane porosity for FSM5, suggesting that further increase in CRHA concentration will not favor an increase in water flux and membrane porosity [10]. Similar trend was reported by Kiani et al., [25] for PET/XA membrane, Nalatambi et al., [30] for CS/GO membrane, Harun et al., [27] for PSF/crystalline rice husk silica and Mulyati et al., [10] for PET/CA/SiO₂ membrane. Apart from membrane porosity factor, another factor contributing to low PWF is the agglomeration of CRHA within the membrane pores and surfaces [30]. This agglomeration can prevent the movement of water molecules across the membranes leading to lower PWF. Hence, FSM2, FSM3 and FSM5 having reduced hydrophilicity as a result CRHA agglomeration on membrane surface.

Table 5: PWF of different membrane samples

Pressure (bar)	Water flux (L/m ² h)				
	FSM1	FSM2	FSM3	FSM4	FSM5
0.5	680.54	200.54	180.63	830.14	700.54
1.0	870.21	350.18	200.50	1100.63	860.30
1.5	1000.24	390.73	280.34	1190.21	1100.46
2.0	1100.38	470.24	330.51	1260.40	1200.08
2.5	1180.46	500.83	420.37	1380.24	1270.54
3.0	1220.34	650.73	590.20	1500.62	1360.30

3.2.2 Oily wastewater filtration experiment

Synthesized oil wastewater from Section 2.4 was used as the feed to evaluate FSM performance in terms of permeate flux and percentage oil rejection during the filtration experiment. Again, dead end filtration apparatus was employed here. Fig. 4 shows the permeate flux of FSM samples with different concentration of CRHA. The permeate flux of different membrane samples initially decreased, reached a steady state condition as time increases. The decline in permeate flux was due to concentration polarization and membrane fouling caused by the blockage of membrane pore space with oil droplet/contaminants [25]. Permeate flux had direct relationship with morphology and porosity of the membrane. Increasing the concentration of CRHA from 0 to 3 wt% caused a decrease in membrane porosity which invariably decreases the membrane permeate flux. Subsequent increase in CRHA concentration led to an increase in membrane porosity as well as the permeate flux, with FSM4 (4 wt% CRHA) having the highest permeate flux of 810 L/m².h at 20 min of filtration. However, FSM5 having 5 wt% CRHA concentrations had lower permeation flux when compared to FSM4 due to reduced membrane porosity.

Fig. 5 shows the percentage oil rejection for different membrane samples. According to the results, percentage (%) oil rejection decreases with an increase in filtration time for all membrane samples. So, increasing CRHA concentration from 0 wt% to 2 wt%, percentage oil rejection increased from 62.17 % to 70.15 % at 20 min filtration time. The high % oil rejection obtained for FSM2 was due to its high water adsorption capacity (53.17%) and reduced membrane pore size. Then, increasing the CRHA concentration from 2 wt% to 3 wt% subsequently decreased the % oil rejection to 58.37 % as a result of decreased membrane porosity, hydrophilicity and water adsorption capacity. Further increase in the concentration of CRHA for FSM4 led to an increase in % oil rejection to a value of 69.42 %. This was attributed to an increase in the transport of water molecules through the membrane pores against oil molecules [25], hence increasing percentage oil rejection. While for FSM5 % oil rejection decreased as a result of decreased membrane porosity and water adsorption capacity. However, the highest percentage oil rejection was recorded for FSM2 and FSM4.

Ultrafiltration of oily wastewater had been reported previously by Al-Ameri & Al-Alawy [35] using hollow fiber PVC membrane. Al-Ameri & Al-Alawy [35] reported permeate flux and % oil rejection of 624.6 L/m².h and 96.6 % respectively. Comparing these values with that obtained in this study, the highest permeate flux & % oil rejection obtained in this study and in that of Al-Ameri & Al-Alawy [35] were 810 L/m².h & 70.15% and 624.6 L/m².h & 96.6 % respectively. However, the flux of the former was higher than that of the later while the % oil rejection of the later was higher than that of the former. But in the present study, FSM2 provided approximately similar flux with that reported by Al-Ameri & Al-Alawy [35]. The disparity observed in the values of flux and % oil rejection reported from these works could be attributed to different materials/method of membrane production.

Conclusively, the addition of CRHA enhanced the permeate flux and % oil rejection in the hybrid PET/PEG/CRHA membrane. These improvements in flux and % oil rejection were attributed to change in membrane morphology and presence of more hydrophilic group of CRHA additive.

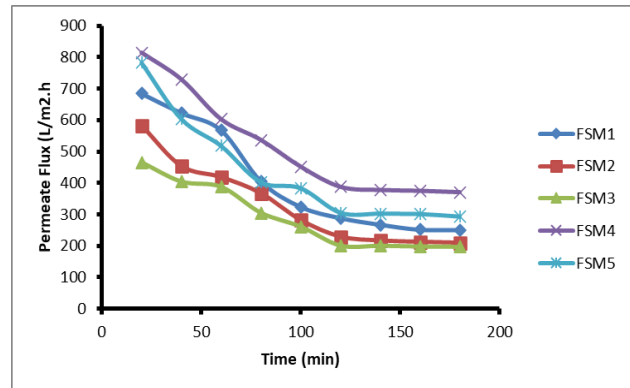


Fig. 4: Permeate flux at varied filtration time for different membrane samples

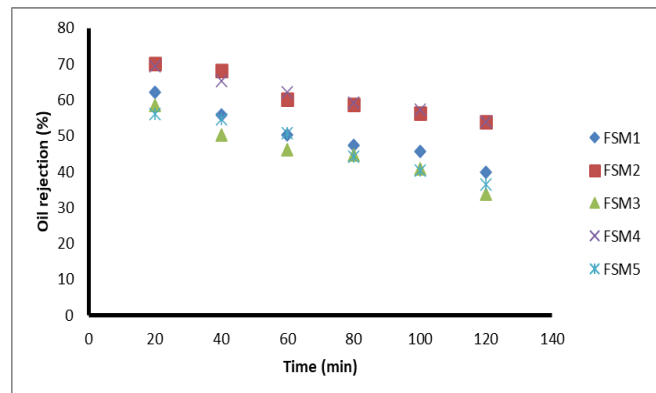


Fig. 5: Percentage oil rejection at varied filtration time for different membrane samples

4.0 Conclusion

In this work, it was established that the synthesized PET/PEG/CRHA membrane samples were successfully used for the ultra-filtration of oily wastewater. Pore forming CRHA was used as an additive to enhance the membrane pore properties, mechanical and thermal stability, hydrophilicity and filtration performances. The characterization results of the various membrane samples indicated that the addition of CRHA into the dope membrane solution significantly influenced the morphological (porosity, pore size, pore distribution and hydrophilicity as seen in the SEM analysis) as well as the performance (permeate flux and percentage oil rejection) characteristics of the produced membrane samples. It was deduced that FSM4 with 4 wt% of CRHA perform optimally well when compared with other FSM samples. It was equally observed that PWF increased with increase in pressure for the various membrane samples. Additionally, PWF initially decreased with increase in CRHA concentration for FSM2 and FSM3, and subsequently increasing the CRHA concentration in

the polymer solution for FSM4 and FSM5 increased the PWF with the highest value of 1500.62 L/m²h recorded in FSM4 at 3.0 bar. While the permeate flux and percentage oil rejection decreased with increasing filtration time for all membrane samples. FSM4 and FSM5 were found to record the highest permeate flux of 813.8 L/m².h and 782.5 L/m².h respectively, while FSM2 and FSM4 recorded the highest percentage oil rejection of 70.15 % and 69.42 % respectively at 20 mins of filtration time. Therefore, it can be concluded that waste plastics bottles (main polymer) and Rice husk ash (additive) can be managed/recycled by reusing these materials for the synthesis of low-cost PET/PEG/CRHA ultra-filtration membranes with improved permeate flux and % oil rejection for the effective treatment of oily wastewater.

References

- [1] Barambu, N. U., Bilad, M. R., Bustam, M. A., Kurnia, K. A., Othman, M. H. D., & Nordin, N. A. H. M. (2021). Development of membrane material for oily wastewater treatment: A review. *Ain Shams Engineering Journal*, 12(2), 1361-1374.
- [2] Anurangi, W. (2011). *Natural and Waste Materials as Adsorbents in Oil Pollution Management*.
- [3] Nuhu, M. M., Rene, E. R., & Ishaq, A. (2022). Remediation of crude oil spill sites in Nigeria: problems, technologies, and future prospects. *Environmental Quality Management*, 31(4), 165-175.
- [4] Abuhasel, K., Kchaou, M., Alquraish, M., Munusamy, Y., & Jeng, Y. T. (2021). Oily wastewater treatment: Overview of conventional and modern methods, challenges, and future opportunities. *Water*, 13(7), 980.
- [5] Putatunda, S., Bhattacharya, S., Sen, D., & Bhattacharjee, C. (2019). A review on the application of different treatment processes for emulsified oily wastewater. *International journal of environmental science and technology*, 16, 2525-2536.
- [6] Tawalbeh, M., Al Mojilly, A., Al-Othman, A., & Hilal, N. (2018). Membrane separation as a pre-treatment process for oily saline water. *Desalination*, 447, 182-202.
- [7] Tanudjaja, H. J., Hejase, C. A., Tarabara, V. V., Fane, A. G., & Chew, J. W. (2019). Membrane-based separation for oily wastewater: A practical perspective. *Water research*, 156, 347-365.
- [8] Muppalla, R., Jewrajka, S. K., & Reddy, A. (2015). Fouling resistant nanofiltration membranes for the separation of oil-water emulsion and micropollutants from water. *Separation and Purification Technology*, 143, 125-134.
- [9] Salahi, A., Noshadi, I., Badrmezhad, R., Kanjilal, B., & Mohammadi, T. (2013). Nano-porous membrane process for oily wastewater treatment: Optimization using response surface methodology. *Journal of Environmental Chemical Engineering*, 1(3), 218-225.
- [10] Mulyati, S., Armando, M., Mawardi, H., Fahrina, A., Malahayati, N., & Syawaliah, S. (2018). Fabrication of hydrophilic and strong pet-based membrane from wasted plastic bottle. *Rasayan J. Chem*, 11, 1609-1617.
- [11] Yalwaji, B., John-Nwagwu, H. O., & Sogbanmu, T. O. (2022). Plastic pollution in the environment in Nigeria: a rapid systematic review of the sources, distribution, research gaps and policy needs. *Scientific African*, 16, e01220.
- [12] Kumartasli, S., & Avinc, O. (2020). Important step in sustainability: polyethylene terephthalate recycling and the recent developments. *Sustainability in the Textile and Apparel Industries: Sourcing Synthetic and Novel Alternative Raw Materials*, 1-19.
- [13] Rajesh, S., & Murthy, Z. V. P. (2014). Ultrafiltration membranes from waste polyethylene terephthalate and additives: synthesis and characterization. *Química Nova*, 37, 653-657.
- [14] Muchtar, S., Wahab, M. Y., Mulyati, S., Arahman, N., & Riza, M. (2019). Superior fouling resistant PVDF membrane with enhanced filtration performance fabricated by combined blending and the self-polymerization approach of dopamine. *Journal of Water Process Engineering*, 28, 293-299.
- [15] Gohari, R. J., Halakoo, E., Nazri, N., Lau, W., Matsuura, T., & Ismail, A. (2014). Improving performance and antifouling capability of PES UF membranes via blending with highly hydrophilic hydrous manganese dioxide nanoparticles. *Desalination*, 335(1), 87-95.
- [16] Arahman, N., Mulyati, S., Lubis, M. R., Razi, F., Takagi, R., & Matsuyama, H. (2016). Modification of polyethersulfone hollow fiber membrane with different polymeric additives. *Membr. Water Treat*, 7(4), 355-365.
- [17] Garcia-Ivars, J., Iborra-Clar, M.-I., Alcaina-Miranda, M.-I., Mendoza-Roca, J.-A., & Pastor-Alcañiz, L. (2014). Development of fouling-resistant polyethersulfone ultrafiltration membranes via surface UV photografting with polyethylene glycol/aluminum oxide nanoparticles. *Separation and Purification Technology*, 135, 88-99.
- [18] Nasrollahi, N., Aber, S., Vatanpour, V., & Mahmoodi, N. M. (2019). Development of hydrophilic microporous PES ultrafiltration membrane containing CuO nanoparticles with improved antifouling and separation performance. *Materials Chemistry and Physics*, 222, 338-350.
- [19] Shen, J., Kaur, I., Baktash, M. M., He, Z., & Ni, Y. (2013). A combined process of activated carbon adsorption, ion exchange resin treatment and membrane concentration for recovery of dissolved organics in pre-hydrolysis liquor of the kraft-based dissolving pulp production process. *Bioresource technology*, 127, 59-65.
- [20] Jamalludin, M. R., Harun, Z., Hubadillah, S. K., Basri, H., Ismail, A. F., Othman, M. H. D., . . . Yunos, M. Z. (2016). Antifouling polysulfone membranes blended with green SiO₂ from rice husk ash (RHA) for humic acid separation. *Chemical Engineering Research and Design*, 114, 268-279.
- [21] Wahab, M. Y., Muchtar, S., Jeon, S., Fang, L. F., Rajabzadeh, S., Takagi, R., . . . Matsuyama, H. (2019). Synergistic effects of organic and inorganic additives in preparation of composite poly (vinylidene fluoride) antifouling ultrafiltration membranes. *Journal of Applied Polymer Science*, 136(27), 47737.
- [22] Olawale, O., & Oyawale, F. A. (2012). Characterization of rice husk via atomic absorption spectrophotometer for optimal silica production. *International Journal of science and Technology*, 2(4), 210-213.
- [23] Kusumocahyo, S. P., Ambani, S. K., Kusumadewi, S., Sutanto, H., Widiputri, D. I., & Kartawiria, I. S. (2020). Utilization of used polyethylene terephthalate (PET) bottles for the development of ultrafiltration membrane. *Journal of Environmental Chemical Engineering*, 8(6), 104381.
- [24] Kusumocahyo, S. P., Ambani, S. K., & Marceline, S. (2021). Improved permeate flux and rejection of ultrafiltration membranes prepared from polyethylene terephthalate (PET) bottle waste. *Sustainable Environment Research*, 31, 1-11.
- [25] Kiani, S., Mousavi, S. M., & Bidaki, A. (2021). Preparation of polyethylene terephthalate/xanthan nanofiltration membranes using recycled bottles for removal of diltiazem from aqueous solution. *Journal of Cleaner Production*, 314, 128082.
- [26] Pereira, A. P. d. S., Silva, M. H. P. d., Lima, É. P., Paula, A. d. S., & Tommasini, F. J. (2017). Processing and characterization of PET composites reinforced with geopolymer concrete waste. *Materials Research*, 20, 411-420.
- [27] Harun, Z., Shohur, M. F., Jamalludin, M. R., Yunos, M. Z., & Basri, H. (2014). Hydrophilicity effect of rice husk silica on mixed

matrix PSF membrane properties. *Jurnal Teknologi*, 70(2), 15-18.

[28] Muhamad, M. S., Salim, M. R., & Lau, W.-J. (2015). Preparation and characterization of PES/SiO₂ composite ultrafiltration membrane for advanced water treatment. *Korean Journal of Chemical Engineering*, 32, 2319-2329.

[29] Ahmad, A., Majid, M., & Ooi, B. (2011). Functionalized PSf/SiO₂ nanocomposite membrane for oil-in-water emulsion separation. *Desalination*, 268(1-3), 266-269.

[30] Nalatambi, S., Oh, K. S., Yoon, L. W., & Tee, L. H. (2023). Evaluation of antibacterial property and greywater treatment performance using composite chitosan/graphene oxide membrane. *Materials Chemistry and Physics*, 295, 127160.

[31] Gola, A., Knysak, T., Mucha, I., & Musiał, W. (2023). Synthesis, Thermogravimetric Analysis, and Kinetic Study of Poly-N-Isopropylacrylamide with Varied Initiator Content. *Polymers*, 15(11), 2427.

[32] Rojjanapinun, A., & Pagsuyoin, S. A. (2021). Rice husk ash and Zr-MOF nanoparticles improve the properties and ultrafiltration performance of PVDF nanomembranes. *Results in Materials*, 12, 100234.

[33] Kiani, S., Mousavi, S. M., Saljoughi, E., & Shahtahmassebi, N. (2018). Preparation and characterization of modified polyphenylsulfone membranes with hydrophilic property for filtration of aqueous media. *Polymers for Advanced Technologies*, 29(6), 1632-1648.

[34] You, P., Kamarudin, S., & Masdar, M. (2019). Improved performance of sulfonated polyimide composite membranes with rice husk ash as a bio-filler for application in direct methanol fuel cells. *International journal of hydrogen energy*, 44(3), 1857-1866.

[35] Al-Ameri, M. K., & Al-Alawy, A. F. (2016). Ultrafiltration of simulated oily wastewater using the method of taguchi. *Int. J. Sci. Eng. Res.*, 7, 503-508.